Time-varying Cost of Distancing: Distancing Fatigue and Lockdowns*

Christoph Carnehl† Satoshi Fukuda‡ Nenad Kos§

May 5, 2026

Abstract

We study a behavioral SIR model with time-varying costs of distancing. We explore the consequences of distancing fatigue and public policies. For a second wave to arise, a steep increase in distancing cost is necessary. We introduce prudent distancing fatigue and show that it cannot trigger a second wave. Both prevalence and fatigue are single-peaked, with fatigue peaking after prevalence. However, policy changes that discontinuously increase distancing costs can cause a second wave, and we characterize the largest such change that avoids it. Finally, numerical analysis shows that an early strict lockdown can have unintended adverse effects.

Keywords: Social Distancing; Distancing Cost; Distancing Fatigue; Second Wave; Lockdown; Lockdown Effectiveness
JEL Classification Numbers: I12; I18; C73

*We thank David McAdams, Jerome Adda, Attila Ambrus, Chantal Marlats, and Lucie Menager for helpful discussions. We also thank seminar participants at SUNY Buffalo for helpful comments.
†Bocconi University, Department of Economics and IGIER. Email: christoph.carnehl@unibocconi.it.
‡Santa Clara University, Leavey School of Business, Department of Economics. Email: sfukuda@scu.edu.
§Bocconi University, Department of Economics, IGIER and CEPR. Email: nenad.kos@unibocconi.it.

1 Introduction

During an epidemic, individuals face risks to their health—and potentially to their lives—as each social interaction may result in infection. To protect themselves, they often reduce their social contacts. Two key factors shape this preventive behavior: the likelihood of infection and the cost of social distancing. This paper examines how changes in the cost of distancing affect individual behavior and, in turn, the dynamics of disease spread.

The reasons for variations in distancing cost are numerous. For example, distancing fatigue leads to a gradual increase in distancing cost as individuals deprive themselves of social interaction. WHO (2020) defines "pandemic fatigue" as demotivation to follow recommended protective behaviors, emerging gradually over time.[1] Franzen and Wöhner (2021) document distancing fatigue among young adults in Switzerland during the COVID-19 pandemic.[2] Religious or seasonal festivals make it more difficult for people to avoid social interactions and, thus, correspond to a sudden and short-term rise in distancing cost.[3] Government policies enacted during an epidemic effectively decrease the distancing cost. For example, closures of restaurants and movie theaters reduce the availability of activities with individuals interacting and thereby encourage social distancing. Conversely, lifting such a policy increases the distancing cost. Hatchett et al. (2007), Bootsma and Ferguson (2007), and Caley et al. (2008) demonstrate that relaxations in non-pharmaceutical interventions increased social activity during the 1918 influenza pandemic. Nguyen et al. (2020) find an increase in mobility soon after US-states reopened during the COVID-19 pandemic.

There is growing evidence that distancing fatigue reduces the effectiveness of a mitigation policy. Goldstein, Yeyati, and Sartorio (2021) show that after four months of lockdown during the COVID-19 pandemic, non-pharmaceutical interventions had a significantly lower effect on reducing fatalities. Petherick et al. (2021) document a decline in the adherence to protective behaviors against COVID-19 in 2020 from a sample of 14 countries. Joshi and Musalem (2021) document larger reductions in mobility during

[1] The root of distancing fatigue can be traced to research documenting how social groups increase the well-being of individuals by offering safety and increased odds of survival. See, for instance, Harlow and Zimmermann (1959), Bowlby (1969), Baumeister and Leary (1995), Eisenberger (2012), and Matthews et al. (2016). Adda, Boucekkine, and Thuilliez (2024) show that policy-induced reductions in mobility have a negative effect on mental health.

[2] There is growing evidence that distancing fatigue reduces the effectiveness of a mitigation policy. See, for instance, Goldstein, Yeyati, and Sartorio (2021), Joshi and Musalem (2021), Petherick et al. (2021) and Du et al. (2022).

[3] According to the American Automobile Association, nearly 56 million people traveled during the 2019 Thanksgiving (https://newsroom.aaa.com/2022/11/thanksgiving-travel-ticks-up-just-shy-of-pre-pandemic-levels/). The Chinese New Year may have been "the biggest human migration on the planet" (https://edition.cnn.com/travel/article/lunar-new-year-travel-rush-2019/index.html), at least until 2019.

the COVID-19 pandemic, while lockdowns remain in place, are associated with higher levels of fatigue. Du et al. (2022) attribute distancing fatigue to a potential reason for the reduced impacts of non-pharmaceutical interventions in the fourth COVID-19 wave in Hong Kong in October 2020.

Motivated by the empirical work outlined above, we explore an SIR (susceptible-infected-recovered) epidemiological model in which myopic individuals choose how much to distance while the distancing cost may change over time in the context of distancing fatigue and public policies. We introduce a model of prudent distancing fatigue, in which the cost of distancing increases gradually in the discounted amount of past distancing. We show that the prevalence remains single-peaked. After the prevalence peaks first, the growth of fatigue slows down up to the point at which fatigue starts decreasing. As a consequence, a second wave of the infection cannot arise from prudent distancing fatigue alone. This reasoning implies that the fatigue itself is also single-peaked and that it peaks after the prevalence. While under prudent distancing fatigue the prevalence remains single-peaked, distancing fatigue heightens peak prevalence potentially burdening the health care system.

While prudent distancing fatigue cannot cause a second wave of an epidemic, a sharp, sudden rise in the cost of distancing can. Public holidays and festivities (when it becomes challenging for individuals to keep social interactions low) or the termination of a mitigation policy (when the distancing cost discretely rises) can generate such sharp increases. To better understand the implications of these increases, we characterize a threshold distancing cost function: by how much would, at each point in time, the distancing cost have to increase or decrease instantaneously to change the sign of the slope of prevalence.

The threshold distancing cost is particularly useful for two purposes. First, when the prevalence is increasing, our characterization shows how much the cost of distancing would have to fall for the prevalence to start decreasing. This information is crucial for a policymaker weighing the harshness of non-pharmaceutical interventions in an attempt to reverse the course of an epidemic. Second, when the prevalence is decreasing, it determines the largest amount by which the distancing cost could increase without causing a second wave, thereby providing vital information for a policymaker considering to lift a mitigation policy. If policymakers base their decisions to relax policies solely on current prevalence and immunity without considering the impact of distancing fatigue, an unintended second wave may arise. Indeed, the epidemiologist Marc Lipsitch argued in April 2020 that the second wave in the fall to be caused by seasonal changes would lead to tighter and costlier social distancing, as he put it: "We will have a harder time controlling coronavirus in the fall ... and we will all be very tired of social distancing and

other tactics."[4]

We conduct a numerical analysis, drawing parallels with the COVID-19 lockdown in China, on the impact of the interplay between a stringent lockdown during the initial phase of an epidemic and prudent distancing fatigue. We find that such a lockdown can lead to a greater total number of infections compared to a scenario without a lockdown. The lockdown at the beginning of an epidemic postpones the spread of the infection. Once it is lifted, individuals have accumulated a substantial level of distancing fatigue. As a consequence, lifting the lockdown leads to less endogenous protective distancing and thus more social interactions than without a prior lockdown. Thus, the combination of distancing fatigue and the sharp rise in distancing cost once the lockdown is lifted, can trigger a severe second wave of the epidemic causing a greater total amount of infections.

Finally, we illustrate how our model with a time-varying distancing cost can be applied to compute the required policy measures affecting individuals' incentives to distance, such as restaurant closures, to achieve a desired transmission rate. While several papers have studied the optimal transmission rate, our model takes into account endogenous distancing choices responding to flexible and time-varying policy measures.

Related Literature. To the best of our knowledge, this is the first paper to study the effects of a time-varying cost of distancing in an SIR model with behavior and establish analytical results about the dynamics of the disease.

The building blocks of the SIR model were set by the seminal work of Ross and Hudson (1917) and Kermack and McKendrick (1927). The incorporation of preventive behavior is more recent. Reluga (2010), Fenichel et al. (2011), Chen (2012), and Fenichel (2013) introduced social distancing into SIR models and provided numerical analyses of equilibrium trajectories.

The assumption of myopic decision-making in SIR models has recently been leveraged to make the analysis more tractable. Engle et al. (2021) propose a behavioral SIR model with myopic agents but with meeting rates that vary across individuals. Dasaratha (2023) analyzes a model where the individuals are uncertain whether they are infected. Carnehl, Fukuda, and Kos (2023) establish that due to the preventive behavior the peak prevalence is non-monotonic in the transmission rate. Their model, unlike the one here, does not allow for variation in the cost of distancing. Avery (2024) studies the interplay between distancing behavior and the willingness to get vaccinated. He models fatigue as an increase in the cost of distancing after a certain amount of time, independently of the previous amount of distancing. McAdams (2021) highlights the advantages of the myopic

[4]https://edhub.ama-assn.org/jn-learning/audio-player/18468053 (Last accessed: January 4, 2024).

approach and provides an excellent review of the literature.[5]

A strand of literature argues that behavioral SIR models without additional time variation cannot fit the path of the COVID-19 pandemic. Droste and Stock (2021) document that a strong self-protective response during the early months of the pandemic was followed by a close-to-zero response during summer. Atkeson et al. (2021) argue that "pandemic fatigue," a decline in the strength of the behavioral response, explains the second wave of infections and deaths in the late fall and winter.[6] Our contribution is to provide a micro-founded behavioral SIR model with distancing fatigue. Our paper also sheds light on how distancing fatigue and public policies change distancing costs and may lead to the second wave.

Papers such as Brett and Rohani (2020), Gualtieri and Hecht (2021), MacDonald, Browne, and Gulbudak (2021), and Meacci and Primicerio (2021) have proposed non-behavioral SIR models to study the effect of epidemic fatigue on the dynamics of an epidemic. Roughly, such non-behavioral SIR models introduce a new compartment that corresponds to epidemic fatigue (e.g., a new susceptible compartment with a higher transmission rate due to fatigue). Our contribution is to study distancing fatigue within a behavioral SIR model. To the best of our knowledge, our paper is the first one that incorporates distancing fatigue into a behavioral SIR model.

Other papers have studied possibilities and reasons behind a second wave. Rachel (2025) argues that lifting a mitigation policy can lead to a second wave without modeling changes in distancing cost.[7] Numerical projections for the COVID-19 pandemic in Giannitsarou, Kissler, and Toxvaerd (2021) suggest that waning immunity can cause several waves. Cochrane (2020) demonstrates that multiple waves of infection may occur when individuals react not to prevalence but to the current death rate, which lags behind prevalence. Goodkin-Gold et al. (2024) consider a model without distancing behavior with vaccinations reducing the number of susceptible individuals. Our paper differs from those by introducing a new channel, variation in the distancing cost.

[5] McAdams, Song, and Zou (2023) study a model with fully forward looking individuals where each individual's distancing cost varies over time because it depends on other non-infected individuals' distancing.

[6] On a related point, Weitz et al. (2020) argue that incorporating fatigue in an epidemiological model can explain multiple waves of infections.

[7] McAdams and Day (2025) endogenize lockdown policies as the outcome of a political process, where political incentives to enforce a lockdown change over time.

2 Model

A continuum of individuals, indexed by $i \in [0,1]$, is infinitely lived with time labeled by $t \in [0,\infty)$. The population is divided into three compartments: susceptible (S), infected (I) and recovered (R). Susceptible individuals can get infected by meeting an infected individual. Infected individuals recover at rate $\gamma > 0$. This implies that it takes on average $1/\gamma$ units of time to recover. After recovery, individuals acquire permanent immunity and cannot get infected again. The size of the population is constant over time: $S(t) + I(t) + R(t) = 1$ for all $t \geq 0$.

Individuals are responsive to the threat of infection and thus might try to avoid it. We capture this by letting a susceptible individual i choose the level of exposure to the infection $\varepsilon_i(t) \in [0,1]$ at each point in time. The susceptible individual who chooses exposure $\varepsilon_i(t)$ at time t gets infected at rate $\beta\varepsilon_i(t)I(t)$, where $\beta > \gamma$ is the transmission rate of the disease. Less exposure, i.e., lower $\varepsilon_i(t)$, decreases the chance of infection. In the absence of the epidemic, the individual would go about her daily business with $\varepsilon_i(t) = 1$. Conversely, we define i's distancing at time t as $d_i(t) := 1 - \varepsilon_i(t)$. We assume that getting infected comes at a cost $\eta \geq 0$ while being susceptible generates a flow payoff of π_S. The assumption that the cost of infection is constant over time is akin to assuming that the individuals are myopic.[8] The standard non-behavioral SIR model corresponds to the case with $\eta = 0$. A reduction in exposure comes at a cost $c_i(t)Q(1-\varepsilon_i(t))$, where $Q : [0,1] \to [0,\infty)$ is increasing, strictly convex, and analytic with $Q'(0) = 0$ and $Q''' \leq 0$.[9] While the marginal distancing cost is growing (i.e., $Q'' > 0$), the rate of that growth is either constant or slowing down (i.e., $Q''' \leq 0$): as an individual approaches total isolation, the additional difficulty of those last few increments does not explode. For instance, the commonly used cost function $Q(d) = \frac{1}{2}d^2$ satisfies these assumptions.[10] The novelty of our model is that we allow individual i's *distancing cost* $c_i(t)$ to vary over time.

More precisely, for each susceptible individual i, the distancing cost is assumed to be

[8] This approach has been frequently adopted in the recent theoretical literature on equilibrium social distancing as it allows for a richer set of results. See, for example, Engle et al. (2021), Dasaratha (2023), Carnehl, Fukuda, and Kos (2023), and Avery (2024). In contrast, in the model with farsighted individuals, the cost of infection η serves as a co-state variable (to the probability of being susceptible), which varies over time. We formally illustrate this point in Appendix B.

[9] An analytic function can be represented by the Taylor series around each point. When the system of differential equations that characterize our behavioral SIR model are analytic, the solution can (analytically and numerically) be solved by Taylor series locally at each point in time.

[10] We require the assumption on the third derivative, $Q''' \leq 0$, only to prove our main result on distancing fatigue, Proposition 2. With non-positive third derivative our model still nests many alternative cost functions. Examples are: (i) $Q(d) = a \cdot d^3 + b \cdot d^2$ with $a \leq 0$ and $b > -3a$; (ii) $Q(d) = a \cdot d \cdot \log(1 + b \cdot d)$ with $a, b > 0$; (iii) $Q(d) = (a \cdot d - \log(1 + a \cdot d))/a^2$ with $a > 0$; and (iv) $Q(d) = (a \cdot d + \exp(-a \cdot d) - 1)/a^2$ with $a > 0$.

a piece-wise continuously differentiable function $c_i : [0, \infty) \to [\underline{c}, \infty)$ with the following three properties: (i) there exists a lower bound $\underline{c} > 0$ such that $c_i(t) \geq \underline{c}$ for all t; (ii) there are at most a finite number of jump discontinuities of c_i, which are common for all individuals i, at $t_1 < \cdots < t_N$ such that, on each interval (t_n, t_{n+1}) with $n \in \{1, \ldots, N\}$,[11] $\dot{c}_i(t)$ is a continuous function satisfying

$$\dot{c}_i(t) = F(t, c_i(t), d_i(t)), \tag{1}$$

where $F(t, \cdot, \cdot)$ is a function of i's current distancing cost $c_i(t)$ and her current distancing level $d_i(t)$; and (iii) at each t_n with $n \in \{1, \ldots, N\}$, c_i is right-continuous. At $t = 0$ and at any point t of jump discontinuity of c_i, the value of $c_i(t)$ is exogenously given and independent of i. In addition, we assume that $c_i(0)$ is independent of i and denote it by c_0. A clarification is in order. While $c_i(t)$ may depend on the identity of an individual i, the environment is symmetric due to the common law of motion F (including the possible jump discontinuities) and the common initial cost c_0. Differences in the cost among individuals might, however, arise due to variations in the choice of distancing.

Two forms of time-varying distancing cost are of particular interest: (i) distancing fatigue—the decline in individuals' willingness to reduce their social activities to prevent infections—and (ii) policy interventions such as restaurant closures and lockdowns. In Section 3, we introduce *prudent distancing fatigue* by having individuals' cost of distancing depend cumulatively on all the previous distancing decisions. Policy interventions are modeled in Section 4 as a reduction in the distancing cost $c_i(t)$.

A susceptible individual i determines her current exposure level by solving:

$$\max_{\varepsilon_i(t) \in [0,1]} \pi_S - c_i(t) Q(1 - \varepsilon_i(t)) - \beta \eta I(t) \varepsilon_i(t). \tag{2}$$

At each time t, the susceptible individual i takes the value of $c_i(t)$ as given, while the resulting exposure level affects the slope of the distancing cost $\dot{c}_i(t)$.[12]

Let the average exposure be $\varepsilon(t) := \frac{1}{S(t)} \int \varepsilon_i(t) di$, where the integral is taken over the susceptible individuals. The disease dynamics are governed by the following system of

[11] For ease of exposition, let $t_{N+1} = \infty$.

[12] Intuitively, consider a discrete-time model in which, at the start of each period, a susceptible individual takes her distancing cost at that time as given. Her resulting exposure level affects her distancing cost at the beginning of the next period. Our model would correspond to the continuous-time limit of such a model.

differential equations:

$$\dot{S}(t) = -\beta\varepsilon(t)I(t)S(t), \tag{3}$$

$$\dot{I}(t) = I(t)(\beta\varepsilon(t)S(t) - \gamma), \tag{4}$$

$$\dot{R}(t) = \gamma I(t), \tag{5}$$

for all except possibly a finite number of t, with the initial condition $(S(0), I(0), R(0)) = (S_0, I_0, 0)$ with $I_0 \in (0, 1)$ and $S_0 = 1 - I_0$. With these in mind, we define an equilibrium.

Definition 1. An *equilibrium* is a tuple of functions $(S, I, R, (c_i, \varepsilon_i)_i)$ with the following three properties: (i) (S, I, R) are continuous functions that satisfy (3), (4) and (5) with the initial condition $(S(0), I(0), R(0)) = (S_0, I_0, 0)$, where ε is the average exposure;[13] (ii) each ε_i solves (2);[14] and (iii) the distancing cost function c_i satisfies (1), where $d_i = 1 - \varepsilon_i$. An equilibrium is *symmetric* if $\varepsilon = \varepsilon_i$ for all i.

As the susceptible individual's objective function is concave in her exposure level, the first-order condition solves the individual's problem. In equilibrium, $\varepsilon := \varepsilon_i$ and $c := c_i$ for all i since individuals may differ only in the distancing cost $c_i(t)$ and $c_i(0) = c_0$ for all i. Therefore, any equilibrium is symmetric:

$$\varepsilon(t) = \max\left(1 - (Q')^{-1}\left(\frac{\beta\eta I(t)}{c(t)}\right), 0\right). \tag{6}$$

An equilibrium exposure level is lower when the prevalence is higher. Distancing increases in the cost of infection η and the transmission rate β, and decreases in the cost of distancing $c(t)$.

Plugging the expression for exposure (6) into the system of differential equations (3), (4), (5), and (1) leads to the system of differential equations characterizing an equilibrium. Our first benchmark result is the existence and uniqueness of an equilibrium.

Proposition 1. *An equilibrium exists, is unique and symmetric. In the unique equilibrium, the system* (S, I, R) *satisfies* $I_\infty := \lim_{t\to\infty} I(t) = 0$, $S_\infty := \lim_{t\to\infty} S(t) \in \left(0, \frac{\gamma}{\beta}\right)$, *and* $\lim_{t\to\infty} \varepsilon(t) = 1$.

We denote by $(S, I, R, c, \varepsilon)$ the symmetric unique equilibrium. Although the distancing cost function c may have a finite number of jump discontinuities, it can be shown

[13] The assumption of the continuity of (S, I, R) is innocuous in light of our application, as discontinuities of c affect distancing behavior only.

[14] That is, ε_i is a best response to (S, I, R) given c_i

that, on each interval (t_n, t_{n+1}), the system of differential equations admits a unique solution $(S, I, R, c, \varepsilon)$. Since (S, I, R) is continuous, the jump discontinuities of c are exogenously given, and since ε follows (6), it follows that an equilibrium exists, is unique, and is symmetric. Since (3) implies that S is non-increasing, the final size of susceptibles S_∞ is well-defined. In the limit, the prevalence disappears and individuals return to full exposure. Similarly to, but extending, behavioral SIR models with a constant distancing cost such as Carnehl, Fukuda, and Kos (2023, Lemma 3), we show that the final size S_∞ is positive and below the threshold of herd immunity $\frac{\gamma}{\beta}$. Thus, some individuals never become infected: $1 - S_\infty < 1$.

Henceforth, we focus on the case in which the prevalence is increasing at the outset: $\dot{I}(0) > 0$. Substituting (6) into (4) at time $t = 0$, this occurs whenever

$$\beta S_0 \left(1 - (Q')^{-1}\left(\frac{\beta \eta I_0}{c_0}\right)\right) - \gamma > 0,$$

which is satisfied as long as the initial seed of infection I_0 is small enough.

3 Continuous Distancing Cost and Prudent Distancing Fatigue

This section studies the case in which the distancing cost is a continuous function of time. Section 3.1 provides a general sufficient condition for an epidemic to be single-peaked. Section 3.2 introduces and investigates a model of prudent distancing fatigue. We show that equilibrium prevalence peaks at most once and discuss consequences of prudent distancing fatigue.

3.1 Sufficient Conditions for Single-Peaked Epidemics

A single peak of an epidemic is one of the most prominent qualitative features of the non-behavioral SIR model: see, for example, Brauer and Castillo-Chavez (2012). Here, we examine conditions on the distancing cost such that this feature remains intact.

Lemma 1. *Let c be a continuously differentiable function such that $\dot{c}$ is given by (1) for all $t > 0$. If*

$$\frac{\dot{c}(t)}{c^2(t)} < \frac{\varepsilon^2(t)}{\eta} Q''\left(1 - \varepsilon(t)\right) \text{ for all } t > 0, \tag{7}$$

then, in equilibrium, prevalence I has a single peak.

Loosely speaking, if the distancing cost is growing slowly, in that $\dot{c}/c^2$ is small, then I has only one local maximum. The prevalence either decreases immediately and never picks up or increases from the outset until it reaches the peak and decreases thereafter. The proof argues that for a second wave to arise, the prevalence would first need to attain a local minimum at some time $t > 0$ for which to occur $\dot{I}(t) = 0$ and $\ddot{I}(t) \geq 0$ are necessary. By taking the derivative of $\dot{I}$, the latter requirement can be shown to be equivalent to the inequality (7). Therefore, if (7) holds for all $t > 0$, there can be no local minimum and consequently no second wave. This result nests as special cases the time-invariant distancing cost $c(t) = c_0$, see Carnehl, Fukuda, and Kos (2023), and the (classical) non-behavioral SIR model.[15]

The following subsection applies the above analysis to distancing fatigue and shows that the prevalence is single-peaked in the prudent distancing fatigue model that we introduce below.

3.2 Prudent Distancing Fatigue

Human nature drives people to socialize, making social distancing increasingly challenging over time. This section examines the model with distancing fatigue. In particular, we introduce prudent distancing fatigue following a decision-theoretic axiomatization of the fatigue utility by Baucells and Zhao (2019). Our analysis shows that in a model with endogenous behavior and time-varying costs of distancing, prudent distancing fatigue alone cannot lead to a second wave: that is, the equilibrium prevalence peaks at most once. In the following, peak prevalence refers to a strict local maximum.

We model *prudent distancing fatigue* using the time-varying distancing cost function:

$$c(t) = c_0 + \varphi(t), \tag{8}$$

where the fatigue

$$\varphi(t) := k \int_0^t e^{-r(t-\tau)} g(1 - \varepsilon(\tau)) d\tau \tag{9}$$

increases in past distancing but the effect of past distancing on fatigue decays over time: $g : [0, 1] \to [0, \infty)$ is increasing, analytic, and satisfies $g(0) = 0$. For instance, $g(d) = d$ satisfies these assumptions. The constant $k \geq 0$, the fatigue accumulation rate, captures the rate at which current distancing increases the distancing cost. The fatigue recovery rate, $r > 0$, determines the rate at which the fatigue decays.

[15] Setting $\eta = 0$ implies that the right-hand side of (7) is infinity.

We refer to a model with the time-varying distancing cost defined as $c(t)Q(1-\varepsilon(t))$ where $c(t)$ follows (8) and (9) while $Q(\cdot)$ is increasing, convex, and analytic with $Q'(0)=0$ and $Q'''(\cdot)\leq 0$ as a model with *prudent distancing fatigue*.[16]

Equation (8) implies that the marginal change in the distancing cost satisfies

$$\dot{c}(t) = kg(1-\varepsilon(t)) - r(c(t)-c_0), \tag{10}$$

with the initial condition $c(0)=c_0$. This differential equation is a special case of equation (1) and therefore existence and uniqueness of equilibrium follow from Proposition 1.

The main result of this section is that prudent distancing fatigue alone does not lead to a second wave.

Proposition 2. *Under prudent distancing fatigue, the following hold:*

1. *The prevalence I is single-peaked.*
2. *The fatigue φ and thus the distancing cost c are single-peaked.*
3. *The fatigue φ attains its peak no earlier than the prevalence I.*

For a second peak to arise, the prevalence would have to attain a local minimum after the first peak and then begin to increase again. Our proof shows that for this to occur, it is necessary that the distancing cost increases sufficiently rapidly after the first peak, while the prevalence is decreasing. However, when the prevalence is falling, the growth of fatigue slows down and fatigue may even decrease. Combining this observation with the marginal cost of distancing being weakly concave ($Q'''(\cdot)\leq 0$) implies that after the peak, distancing does not decrease fast enough to jump-start another wave.

To see that prudent fatigue cannot peak before prevalence, note that distancing intensifies at the onset of an epidemic. At any stationary point of fatigue φ, equation (10) implies

$$kg(1-\varepsilon(t)) = r\big(c(t)-c_0\big).$$

Because the excess cost $c(t)-c_0$ is an exponentially discounted average of past values of $g(1-\varepsilon(t))$, this equality can hold at a peak of $c(t)$ only after current distancing has already begun to ease. Hence, distancing must be below its maximal level. Moreover,

[16] We refer to our model of distancing fatigue as *prudent* distancing fatigue, as our assumption that $Q'''(\cdot)\leq 0$ is analogous to standard assumptions in macroeconomics and the economics of uncertainty that assume a positive third derivative on utility functions. In our model, the individual is prudent with respect to her costs of distancing.

for fatigue to be locally declining at the same point (that is, for the stationary point to be a local maximum), $g(1-\varepsilon(t))$ must be falling, which is equivalent to distancing relaxing. But a relaxation of distancing while fatigue is momentarily flat can occur only once prevalence is itself decreasing. Hence, fatigue peaks after the peak of prevalence.

This qualitative implication is important: fatigue may continue to accumulate even after prevalence has begun to decline. Although distancing is already decreasing, it may still remain above its own discounted average since the start of the epidemic. As a result, the fatigue stock can continue to build for some time, albeit only gradually.

In the long term, the distancing cost converges to its initial level, $\lim_{t\to\infty} c(t) = c_0$, and, individuals recover from fatigue, $\lim_{t\to\infty} \varphi(t) = 0$ as the infection dies out.

Our findings suggest that prudent distancing fatigue does not affect qualitative features of the prevalence trajectory. This, however, is not to say that distancing fatigue cannot play an important role in epidemiological models.

First, it may very well have critical quantitative implications. Goldstein, Yeyati, and Sartorio (2021), for example, show that after four months of lockdown during the COVID-19 pandemic, non-pharmaceutical interventions had a significantly lower effect on reducing fatalities. In our model, the peak prevalence in the model with prudent distancing fatigue is always higher than the peak prevalence in the model without it, and the peak prevalence in the model with prudent distancing fatigue is reached no earlier than in the one without it. Thus, distancing fatigue may burden the medical capacity constraint at the peak prevalence.

Second, distancing fatigue introduces two opposing effects on individuals' distancing decisions. On the one hand, when the distancing cost increases due to distancing fatigue, ceteris paribus, the individuals increase their exposure because distancing becomes more costly. On the other hand, higher prevalence due to distancing fatigue makes it more costly for an individual to increase exposure. This second effect decreases individuals' exposure levels. Hence, to measure the effect of distancing fatigue on exposure, it is also important to measure the effect that an increased prevalence has on individuals' preventive behavior.

Third, distancing fatigue introduces a negative dynamic spillover to lockdown policies. By encouraging or enforcing social distancing in the current period, the lockdown reduces distancing incentives in the future due to accumulated distancing fatigue. Holding lockdown stringency fixed, lockdown effectiveness declines over time and the likelihood of a second wave may increase should the lockdown be lifted. Our result that prudent dis-

tancing fatigue alone does not cause the second wave suggests that the second wave may result rather from the discrete increase in distancing cost from lifting the lockdown policy.

4 Policy Interventions

The cost of social distancing depends not only on previous exposure decisions but also on other factors such as public health policies. This section examines the effects of discontinuous policy changes in distancing cost. Specifically, we consider a time-varying policy variable $\ell(t) \in [\underline{c}/c_0, 1]$ with at most finitely many discontinuities such that

$$c_i(t) = c_0 \cdot \ell(t) \in [\underline{c}, c_0], \tag{11}$$

where $\ell(t)$ can be interpreted as the strictness of the policy intervention at time t. While the analysis to follow is cleanest with discontinuous changes, the results do not rely as much on the discontinuity as they do on sudden rapid changes in the cost of distancing. Also, we focus on policy interventions that encourage social distancing behavior by reducing the distancing cost. However, introducing periods of increased distancing cost (i.e., holidays) can be straightforwardly implemented as well by allowing the distancing cost to increase.

We begin by introducing a useful technical tool for assessing whether a policy change can trigger a second wave. Specifically, we characterize a time-t threshold for the distancing cost, $\overline{c}(t)$, with the property that prevalence is locally increasing if $c(t) > \overline{c}(t)$ and locally decreasing if $c(t) < \overline{c}(t)$. The gap $\overline{c}(t) - c(t)$ therefore quantifies the largest *instantaneous* increase in $c(t)$ that leaves the sign of $\dot{I}(t)$ unchanged.

In particular, suppose a policy is in place and the current cost satisfies $c(t) < \overline{c}(t)$, so that $\dot{I}(t) < 0$ and prevalence is declining. Lifting the policy induces an immediate upward jump in c. If, after this jump, the cost remains below $\overline{c}(t)$, prevalence continues to fall. If instead the jump pushes c above $\overline{c}(t)$, the slope of $I(t)$ switches discontinuously from negative to positive—$\dot{I}(t) > 0$—thereby initiating a new wave.

The following definition introduces the threshold distancing cost function $\overline{c}$ and the subsequent proposition formalizes the above intuition.

Definition 2. Let c be a piece-wise continuously-differentiable distancing cost function and let $(S, I, R, c, \varepsilon)$ be the corresponding equilibrium.[17] We define the threshold dis-

[17]Note that (S, I, R) are continuous functions satisfying (3), (4) and (5) with the initial condition

tancing cost function $\overline{c}$ as follows: for each $t \geq 0$,

$$\overline{c}(t) := \begin{cases} \frac{\beta\eta I(t)}{Q'(1-\frac{\gamma}{\beta S(t)})}, & \text{if } S(t) > \frac{\gamma}{\beta} \\ \infty, & \text{if } S(t) \leq \frac{\gamma}{\beta} \end{cases}.$$

Proposition 3. *Let c be a piece-wise continuously-differentiable distancing cost function, and let $\overline{c}$ be the associated threshold distancing cost function. For any $t > 0$ and piece-wise continuously-differentiable distancing cost function c_2 such that the corresponding equilibrium $(S_2, I_2, R_2, c_2, \varepsilon_2)$ satisfies the property that $c_2(s) = c(s)$ for all $s < t$, the following holds:*

$$\dot{I}_2(t_+) := \lim_{\tau \downarrow t} \dot{I}_2(\tau) < 0 \text{ if and only if } c_2(t) < \overline{c}(t).$$

In words, the threshold distancing cost function $\overline{c}$ satisfies the following property. Fix a distancing cost function c and its implied equilibrium, and consider an alternative distancing cost function c_2 that coincides with c up to time t. Then, $\overline{c}(t)$ prescribes the largest value that the distancing cost $c_2(t)$ can take on such that the right-limit of the derivative of $I(t)$ under $c_2(t)$ is negative.[18]

Whenever c is such that I is single-peaked in equilibrium, the threshold distancing-cost function $\overline{c}$ intersects c once and from below. In particular, as long as $\dot{I}(t) > 0$, $\overline{c}(t) < c(t)$ and conversely so if $\dot{I}(t) > 0$. In addition, when $S(t)$ approaches $\frac{\gamma}{\beta}$ from above, $\overline{c}(t)$ grows towards infinity.

The difference $\overline{c} - c$ plays an important role. When the prevalence is decreasing, the cost difference informs by how much the cost can instantaneously increase without the prevalence starting to increase. Conversely, when the prevalence is already increasing, the difference $c - \overline{c}$ establishes by how much the cost of distancing must decrease for the prevalence to start falling. This is of particular interest to policymakers who are trying to establish the strictness of public health policies required to reduce the prevalence immediately. Conversely, it can be used to establish whether lifting a policy will lead to a second wave. Bootsma and Ferguson (2007), Hatchett et al. (2007), and Caley et al. (2008) suggest that, during the 1918 influenza pandemic, relaxations in non-pharmaceutical interventions caused a new surge of cases.

We consider the introduction of a temporary lockdown and show how the threshold

$(S(0), I(0), R(0)) = (S_0, I_0, 0)$, where ε is the average exposure that satisfies (6). The equilibrium is unique and symmetric.

[18] Note that $\overline{c}$ depends on the equilibrium path $(S, I, R, c, \varepsilon)$ under the distancing cost function c.

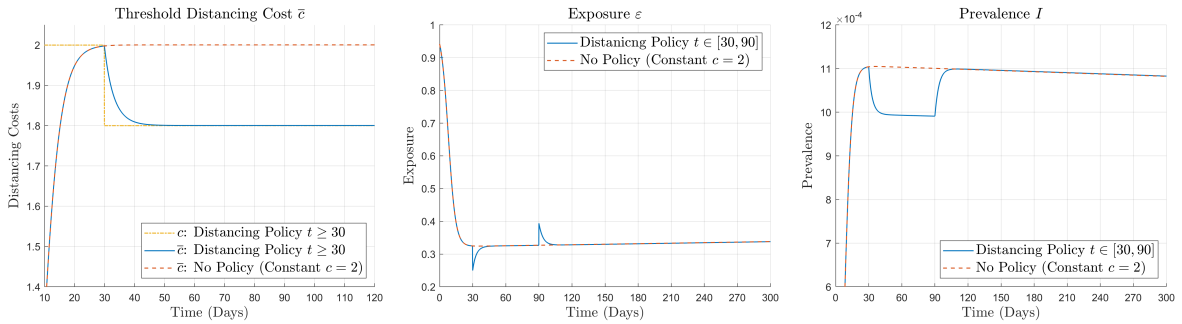

Figure 1: *Social-Distancing Policy.* The left panel depicts the threshold distancing cost function $\bar{c}$ over time. The central panel depicts the exposure level ε over time. The right panel depicts the prevalence I over time.

function $\bar{c}$ can guide policymakers.

Example 1. We consider the introduction of a social-distancing policy. Letting the baseline distancing cost be $c(t) = c_0 = 2$, the dashed curve in the left panel of Figure 1 shows by how much the distancing cost c must be reduced to decrease the prevalence before it would reach its peak otherwise.[19] The threshold cost $\bar{c}(t)$ is 1.8 around day 15 and the peak prevalence is attained on day 35. Suppose that the social-distancing measure $\ell(t) = 0.9$, which decreases distancing cost to $c(t) = 1.8$, is introduced on day 30.

The solid curve in the left panel in Figure 1 gives a new threshold distancing cost function $\bar{c}$ when the distancing cost function satisfies $c(t) = 1.8$ for $t \geq 30$. After the introduction of the social-distancing measure, the prevalence decreases, and the new threshold $\bar{c}$ endogenously decreases as well. The figure shows that on day 50, the threshold cost is close to (but above) the current distancing cost.

To understand the new threshold distancing cost function, consider how individuals respond to the social-distancing measure. As the central panel of Figure 1 shows, individuals best respond to the policy measure by decreasing their exposure levels. The resulting increase in distancing lowers prevalence, which leads to a feedback effect of increasing exposure. The prevalence nevertheless continues to decrease albeit at a slower pace due to the individuals' responses, as illustrated in the right panel of the figure.

After day 50, virtually any easing of the social-distancing measure causes the second wave. For instance, if the distancing measure is lifted in its entirety after two months (i.e., on day 90), the infection resurges, and around day 111, the prevalence almost coincides with the case in which no distancing measure is introduced, as depicted in the right panel

[19] We let $Q(d) = \frac{1}{2}d^2$. We choose the model parameters $(\beta, \gamma, I_0, \pi_S, c_0, \eta)$ based on the parameters calibrated in Carnehl, Fukuda, and Kos (2023), where $c_0 = 2$ is a normalization. See Appendix C for details.

of Figure 1.[20] □

5 Numerical Analysis of Public Policies with Distancing Fatigue

This section combines the two sources of time variation in the distancing cost we study—public policies and prudent distancing fatigue—and demonstrate that distancing fatigue can have adverse effects on a well-intended public policy.

We simulate our model on the basis of numbers motivated by China's strict COVID-19 lockdown and show that a strict lockdown from the outset of the epidemic may increase both the final number of infected individuals and the peak of the prevalence in the second wave arising upon the lifting of the lockdown. The reason is that a lockdown imposed at the beginning of the epidemic, that does not completely eradicate the infection, effectively postpones the spread of the disease until the lifting of the lockdown. At that point, individuals are fatigued and thus reluctant to distance as much as they would have in the absence of the lockdown.

While the analysis based on China's lockdown below is relatively extreme in terms of the strictness and duration of the policy as well as the calibrated fatigue parameters, the insights are more general. Similar qualitative patterns arise from more moderate fatigue parameters and shorter, less strict policies.

Example 2. To illustrate the interaction between fatigue and public policy, we approximate China's COVID-19 lockdown within our model of prudent distancing fatigue. We choose the parameters $(\beta, \gamma, I_0, \eta, c_0)$ based on the ones calibrated in Carnehl, Fukuda, and Kos (2023): see Appendix C for details. We impose a lockdown in the model starting ten days after the epidemic's start. To focus on the effect of distancing fatigue during the lockdown, we assume that individuals' distancing cost is constant before the lockdown is imposed and follows equation (8) afterwards, where $g(d) = d$. We also let $Q(d) = \frac{1}{2}d^2$. For simplicity, we assume that the lockdown lasts for 365 days. The lockdown induces a 75% reduction in social activity in line with the empirical findings in Zhong et al. (2022), who find a 74.1-80% reduction in mobility in China.[21] To obtain reasonable distancing fatigue parameters (k, r) for equation (8), we choose the fatigue parameters such that

[20] A vaccination campaign (i.e., a reduction in S) during a lockdown helps prevent the resurgence of the infection. All else being equal, a reduction in $S(t)$ increases the threshold distancing cost $\bar{c}(t)$ as $\frac{\partial \bar{c}(t)}{\partial S(t)} = -\frac{\beta^2 \eta \gamma I(t)}{(\beta S(t) - \gamma)^2} < 0$.

[21] A time-varying lockdown policy $\ell(t)$ can implement a desired, constant reduction in social activity.

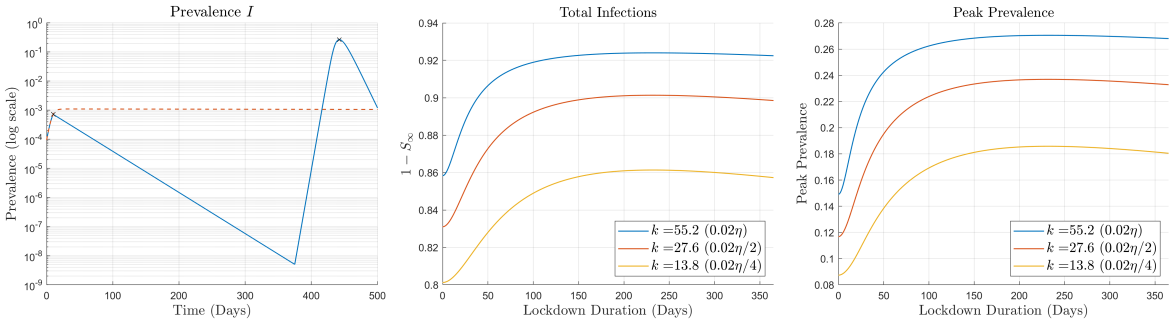

Figure 2: *Lockdown Policy.* The y-axes are truncated to highlight variation. The left panel depicts the prevalence curves with (blue solid curve) and without (red dashed curved) the lockdown on a logarithmic scale. The central panel depicts the total number of infections $(1 - S_\infty)$ as a function of the lockdown duration. The right panel depicts the peak prevalence as a function of the lockdown duration.

the model-predicted peak after the lifting of the lockdown would match the peak of the second wave observed in China. We chose $k = 0.02\eta$ and $r = 0.01$.

The left panel of Figure 2 depicts the prevalence curves under no lockdown policy (dashed) and under the lockdown policy (solid). The prevalence peaks on day 442, approximately two months after the policy is lifted. At the peak, around 27% of individuals are infected. Our simulations show that, at that point, approximately two thirds of the population has been infected.[22]

To understand the role played by the strict lockdown interacting with distancing fatigue, note that the non-behavioral SIR model, which provides an upper bound for the model studied here, predicts the peak prevalence at roughly 31%.[23] In a behavioral SIR model without distancing fatigue, the peak prevalence would be at about 0.1%. Hence, it seems that in a model with both distancing fatigue and a long and strict lockdown the benefits of voluntary social distancing are almost entirely removed.

We can quantify the contribution of the prolonged lockdown on the peak prevalence

[22]This is not far away from the statement made by the chief epidemiologist of China's Center for Disease Control and Prevention that the "epidemic has already infected about 80% of the people" in China as of January 21, 2023 (https://edition.cnn.com/2023/01/22/china/china-covid-80-lunar-new-year-intl-hnk/index.html).

[23]A strict, long lockdown leads to high levels of fatigue and thus a high distancing cost upon lifting the lockdown. When $\beta\eta/c(t) \approx 0$, the disease dynamics after the lockdown can be well approximated by the standard non-behavioral SIR model with the post-lockdown initial condition (S_*, I_*) as the share of susceptible individuals is still high as the lockdown was imposed early in the epidemic. This model predicts a peak prevalence of

$$\overline{I} = \frac{\gamma}{\beta} \log\left(\frac{\gamma}{\beta}\right) - \frac{\gamma}{\beta} - \frac{\gamma}{\beta} \log(S_*) + S_* + I_*$$

(see, for instance, Brauer and Castillo-Chavez, 2012). This gives the prevalence of the second peak at 31% as opposed to 27% in our example.

by considering the situation in which the lockdown is not implemented but individuals still accumulate fatigue. In this case, the peak prevalence would be at about 15% (see the right panel of Figure 2). Thus, while fatigue alone accounts for an increase of the peak prevalence from 0.1% to 15%, the prolonged lockdown accounts for an additional increase of the peak prevalence from 15% to 27%, suggesting that the contribution of the prolonged lockdown is substantial.

The central panel of Figure 2 depicts the total number of infections $1 - S_\infty$ and the prevalence at the second peak as a function of the lockdown duration. To see the robustness of the qualitative features of these two measures, we consider three different fatigue accumulation rates $k \in \{0.02\eta, 0.01\eta, 0.005\eta\}$. The other model parameters are fixed. It is striking to see that both the total number of infections $1 - S_\infty$ and the peak prevalence are lowest without any lockdown—they are initially increasing in the lockdown duration. After a certain threshold duration of the lockdown, we observe that while a policy-maker may have preferred to impose a shorter or no lockdown at all, the size of the epidemic and the second peak prevalence can be reduced only by keeping the lockdown in place for an extended period of time.[24] □

This example illustrates the important trade-off between breaking an initial wave of an epidemic with a strict lockdown policy and the cost of lifting the lockdown after individuals have accumulated substantial levels of distancing fatigue.

6 Public Policies as Time-Varying Distancing Cost

In this section, we illustrate how our model with a time-varying cost of distancing can inform policy-making about the optimal path of public policy restrictions to implement a target level of a time-varying transmission rate. Several papers have analyzed optimal mitigation policies in a reduced form by assuming that a planner controls the path of the disease.[25] That is, they assume that a planner directly controls the time-varying transmission rate, $\beta(t)$, or social interactions, $\varepsilon(t)$. Both cases can be viewed as a planner controlling an effective transmission rate $\tilde{\beta}(t) = \beta(t)\varepsilon(t)$, in which either $\beta(t)$ is controlled and $\varepsilon(t)$ is constant or in which β is constant and $\varepsilon(t)$ is controlled.

While mask mandates can directly affect the transmission rate, the attainable levels of

[24] Note, however, that in these simulations, we do not impose any direct lockdown cost and only consider relatively early starting dates of the lockdown.

[25] See, for example, Acemoglu et al. (2021), Alvarez, Argente, and Lippi (2021), Farboodi, Jarosch, and Shimer (2021), Chakrabarti et al. (2022), and Kruse and Strack (2023).

the transmission rate are limited by such a policy alone. Many countries have introduced additional policies beyond mask mandates to reduce transmission during the COVID-19 pandemic. Such policies aim at reducing the spread of the infection via reduced social interactions, such as bar and restaurant closures. However, because policy effectiveness depends on the endogenous social distancing choices of individuals, behavior should be modeled explicitly to account for how these incentives change alongside the epidemic.[26]

Nevertheless, the results obtained in these papers are important to understand the desirable epidemic paths of a planner who optimizes subject to macroeconomic or other cost considerations. These papers typically model behavior only in reduced form through a time varying effective transmission rate $\tilde{\beta}(t)$, which a planner controls. We show how our equilibrium distancing model with a time-varying cost can be used to back out a policy path that affects the cost directly, $c(t)$, to induce the effective reduced-form transmission rate $\tilde{\beta}(t)$. That is, given a path $\tilde{\beta}(t)$, we derive the time-varying cost function $c(t)$ that can implement it, taking endogenous behavioral responses to both the disease and the policies into account.

Consider a desirable time-varying transmission rate $\tilde{\beta}(t)$ for given primitives of the non-behavioral SIR model (i.e., β, γ, I_0, and $S_0 = 1 - I_0$). The dynamics of the disease under the desirable transmission rate function $\tilde{\beta}$ follows the system of equations (3), (4), and (5) where $\beta\varepsilon(t)$ is replaced by $\tilde{\beta}(t)$. Then, we can use our model to solve for the time-varying distancing cost function $\tilde{c}$ implementing the transmission rate function $\tilde{\beta}(t) = \beta\varepsilon(t)$ via

$$\tilde{c}(t) := \frac{\beta\eta I(t)}{Q'\left(\frac{\beta-\tilde{\beta}(t)}{\beta}\right)},$$

provided $\tilde{\beta}(t) < \beta$. Recalling equation (11), without distancing fatigue, the required lockdown severeness $\tilde{\ell}(t)$ follows

$$\tilde{\ell}(t) := \frac{\beta\eta I(t)}{c_0 Q'\left(\frac{\beta-\tilde{\beta}(t)}{\beta}\right)}.$$

However, using equation (8), we can straightforwardly also incorporate distancing

[26] Carnehl, Fukuda, and Kos (2023) show that policies that affect distancing incentives via reductions in the transmission rate and changes in the cost of distancing have qualitatively different effects on the path of an epidemic.

fatigue $\varphi(t)$ to obtain:

$$\tilde{\ell}_{\varphi}(t) := \frac{1}{c_0}\left(\frac{\beta\eta I(t)}{Q'\left(\frac{\beta-\tilde{\beta}(t)}{\beta}\right)} - \varphi(t)\right).$$

It should be noted that there is an endogenous upper bound on the implementable $\tilde{\beta}(t)$, which derives from individuals' endogenous distancing without policy interventions. Unless meetings can be subsidized during an epidemic, that is, more exposure encouraged than individuals would voluntarily engage in, $\tilde{\beta}(t) > \beta$ cannot be attained.

An important observation is that the strictness of the policies in place depends not only on the transmission rate to be implemented but also on current prevalence $I(t)$, fatigue $\varphi(t)$, and the cost of infection η. If the prevalence or the cost of infection is high or if fatigue is low, policies do not have to be as strict to induce a certain transmission rate as otherwise. This suggests that in models studying the optimal control of a transmission rate during an epidemic, the cost function of reducing the transmission rate should at least depend on the current prevalence to take endogenous distancing decisions into account.[27]

Finally, an analogous approach is feasible to implement desired levels of the effective reproduction number $\mathcal{R}^e(t)$ which measures how many secondary infections are caused by each infected individual.[28] Whenever $\mathcal{R}^e(t) > (<)1$, the prevalence is increasing (decreasing). For example, Budish (2025) considers $\mathcal{R}^e(t) \leq 1$ as a constraint for a planner without an explicit dynamic equilibrium model. In our setting, this constraint corresponds to the current policy satisfying the constraint that $c(t) \leq \bar{c}(t)$ as in Proposition 3.

7 Conclusion

This paper introduces a behavioral SIR model with time-varying distancing costs by focusing on two main applications: distancing fatigue and public policies. We incorporate endogenously evolving prudent distancing fatigue into a behavioral SIR model by assuming that individuals' distancing costs increase in their past distancing. We show that prudent distancing fatigue alone cannot cause a second wave of infection. For a second

[27] The distancing cost function $\tilde{c}$ can be interpreted as the ratio between the marginal benefit of distancing $\beta I(t)\eta$ (relative to c_0) and the reduction of the transmission rate $\frac{\beta-\tilde{\beta}(t)}{\beta}$.

[28] In the non-behavioral SIR model, the effective reproduction number is given by $\frac{\beta}{\gamma}S(t)$. In our behavioral SIR model, the effective reproduction number is given by $\frac{\beta\varepsilon(t)}{\gamma}S(t)$.

wave to arise, the distancing cost has to increase rapidly after the first peak. Distancing fatigue postpones the time at which prevalence peaks and raises the level of peak prevalence. Thus, prudent distancing fatigue may still have substantial consequences for the medical system even though the prevalence remains single-peaked.

While prudent distancing fatigue alone does not cause a second wave, changes in public policies can. In particular, the removal of a mitigation policy can induce a sufficient increase in the distancing cost for a second wave to arise. Thus, policymakers must consider the consequences of changes in public policies through behavioral responses carefully. To guide such considerations, we formulate a threshold distancing cost function. If individuals' distancing costs remain below the threshold then the prevalence does not increase.

Finally, we examine the interplay of lockdown policies and distancing fatigue. Crucially, distancing fatigue imposes a negative dynamic spillover on lockdowns. The policy that curtails mobility in the current period reduces distancing incentives in the future via two channels: (i) lower prevalence and (ii) accumulated distancing fatigue. Holding lockdown stringency fixed, distancing fatigue reduces lockdown effectiveness over time, and increases the prevalence level of a second wave should the lockdown be lifted. Consequently, a current lockdown decreases the effectiveness of any future lockdown policies. In addition, we demonstrate that longer lockdowns can cause higher prevalence levels in the second wave—even exceeding the prevalence levels without any lockdown at all.

A Proofs

Proof of Proposition 1. At each time t, an individual's problem (2) is concave. Thus, the first-order condition is sufficient. This pins down the individual's optimal distancing in the SIR dynamics. By the arguments in the main text, an equilibrium is symmetric. Using the exposure obtained from (6) in the SIR dynamics together with the cost-function evolution yields

$$\dot{S}(t) = -\beta S(t) I(t) \max\left(1 - (Q')^{-1}\left(\frac{\eta\beta I(t)}{c(t)}\right), 0\right), \tag{12}$$

$$\dot{I}(t) = \beta S(t) I(t) \max\left(1 - (Q')^{-1}\left(\frac{\eta\beta I(t)}{c(t)}\right), 0\right) - \gamma I(t), \tag{13}$$

$$\dot{R}(t) = \gamma I(t), \tag{14}$$

$$\dot{c}(t) = F\left(t, c(t), \max\left(1 - (Q')^{-1}\left(\frac{\eta\beta I(t)}{c(t)}\right), 0\right)\right), \tag{15}$$

for all but possibly a finite number of t, at which at least one of the variables (S, I, R, c) is not differentiable. Let $t_1 < \cdots < t_N$ be the set of these points (this set may possibly be empty). Let $t_{N+1} = \infty$.

Thus, in any equilibrium, (S, I, R, c) is characterized by the system of differential equations $\frac{d}{dt}(S, I, R, c) = G(t, S, I, R, c)$, where G is defined by (12), (13), (14), and (15). The initial condition is $(S(0), I(0), R(0), c(0)) = (S_0, I_0, 0, c_0)$. Then, the initial value problem admits a unique solution (S, I, R, c) on $[0, t_1)$, as the system satisfies the conditions of the Picard-Lindelöf Theorem. Namely, the function G is continuous on the domain $D = [0, t_1) \times [0, 1]^3 \times [\underline{c}, \infty)$, and G is uniformly Lipschitz continuous in (S, I, R, c): there exists a Lipschitz constant L satisfying $\|G(t, S, I, R, c) - G(t, \tilde{S}, \tilde{I}, \tilde{R}, \tilde{c})\| \leq L\|(S, I, R, c) - (\tilde{S}, \tilde{I}, \tilde{R}, \tilde{c})\|$ for each $t \in [0, t_1)$. See, for example, Walter (1998). Since the equilibrium definition requires S, I and R to be continuous, we apply the same logic to the interval $[t_1, t_2)$ with the initial value $(S(t_1), I(t_1), R(t_1)) = \lim_{t \uparrow t_1}(S(t), I(t), R(t))$ and all the subsequent intervals. Note that each $c(t_n)$ is also given. Now, $\varepsilon = \varepsilon_i$ is uniquely determined, and hence the model admits a unique and symmetric equilibrium.

Next, we show $\lim_{t\to\infty} I(t) = 0$. Since $R(\cdot) \in [0, 1]$ is weakly increasing, $\lim_{t\to\infty} R(t)$ exists in $[0, 1]$. Therefore, $0 = \lim_{t\to\infty} \dot{R}(t) = \gamma \lim_{t\to\infty} I(t)$, where the second equality follows from equation (14). Thus, $I_\infty = 0$.

Next, $\lim_{t\to\infty} \varepsilon(t) = 1$ follows from taking the limit of (6) because the distancing cost is bounded from below, $c(t) \geq \underline{c}$, and $\lim_{t\to\infty} I(t) = 0$.

Finally, having established $\lim_{t\to\infty} I(t) = 0$ and $\lim_{t\to\infty} \varepsilon(t) = 1$, we show that these properties imply $S_\infty \in \left(0, \frac{\gamma}{\beta}\right)$ given the SIR dynamics (3)-(5).

The proof consists of two steps. In the first step, suppose to the contrary that $S_\infty > \frac{\gamma}{\beta}$. Since S is weakly decreasing, there exists $\delta > 0$ such that $S(t) \geq \delta + \frac{\gamma}{\beta}$ for all $t \geq 0$. Since $\lim_{t\to\infty} \varepsilon(t) = 1$ and $\delta > 0$, for a given $\kappa \in (0, \delta)$, there exists $t_1 < \infty$ such that $\delta\varepsilon(t) - \frac{\gamma}{\beta}(1 - \varepsilon(t)) > \kappa$ for all $t \geq t_1$. Then, for all $t \geq t_1$, we have

$$\dot{I}(t) = \beta I(t)(S(t)\varepsilon(t) - \frac{\gamma}{\beta}) \geq \beta I(t)((\delta + \frac{\gamma}{\beta})\varepsilon(t) - \frac{\gamma}{\beta}) > \beta I(t)\kappa, \text{ that is, } \frac{\dot{I}(t)}{I(t)} > \beta\kappa.$$

Thus, $I(t) \geq I(t_1)e^{\beta\kappa(t-t_1)}$, which yields $I_\infty = +\infty$. This is a contradiction to $I_\infty = 0$.

The second step establishes $S_\infty \neq \frac{\gamma}{\beta}$. Suppose to the contrary $S_\infty = \frac{\gamma}{\beta}$. Then,

$\frac{dI}{dS}(S_\infty) = -1 + \frac{\gamma}{\beta}\frac{1}{S_\infty} = 0$ as $\lim_{t\to\infty} \varepsilon(t) = 1$. However, note that

$$\begin{aligned}\frac{d}{dS}\frac{dI}{dS}(S_\infty) &= -\frac{\gamma}{\beta}\frac{1}{\varepsilon(I(S))S}\left(\frac{1}{S} + \frac{1}{\varepsilon(I(S))}\frac{d\varepsilon(I(S))}{dI(S)}\frac{dI}{dS}(S)\right)\Big|_{S=S_\infty} \\ &= -\frac{\gamma}{\beta}\frac{1}{\varepsilon_\infty S_\infty^2} < 0\end{aligned}$$

as $\frac{dI}{dS}(S_\infty) = 0$, where $\varepsilon_\infty = \lim_{t\to\infty} \varepsilon(t) = 1$. Thus, there is a $\delta > 0$ such that for $S \in (S_\infty, S_\infty + \delta)$, $\frac{dI}{dS}(S_\infty + \delta) < 0$ and, hence, that $I(S_\infty + \delta) < 0$, a contradiction. Thus, $S_\infty < \frac{\gamma}{\beta}$. □

Proof of Lemma 1. To have at least two peaks, there must be two local strict maxima of I at $t_2 > t_1 \geq 0$. Because I is continuous it has a minimum on $[t_1, t_2]$ by the extreme-value theorem. Moreover, since t_1 and t_2 are local strict maxima, the minimum has to be attained at some $\hat{t} \in (t_1, t_2)$. The fact that in equilibrium S, I and R are continuous implies that I is differentiable and that its derivative is given by (4).

As I has a local minimum at $\hat{t}$, $\dot{I}(\hat{t}) = 0$ and thus $\beta\varepsilon(\hat{t})S(\hat{t}) = \gamma$. It follows that $\varepsilon(t) > 0$ and $S(t) > 0$ in the neighborhood of $\hat{t}$. Therefore, evaluating $\ddot{I}(t)$ with $\dot{I}(t) = 0$ yields

$$\ddot{I}(t)\Big|_{\dot{I}(t)=0} = \beta I(t)(\dot{\varepsilon}(t)S(t) + \varepsilon(t)\dot{S}(t)). \tag{16}$$

Differentiating ε, we have

$$\dot{\varepsilon}(t) = \frac{1}{Q''(1-\varepsilon(t))}\frac{\beta\eta I(t)}{c(t)}\left(\frac{\dot{c}(t)}{c(t)} - \frac{\dot{I}(t)}{I(t)}\right).$$

Substituting the latter equality and $\dot{S}(t) = -\beta\varepsilon(t)I(t)S(t)$ into (16) results in

$$\ddot{I}(t)\Big|_{\dot{I}(t)=0} = \beta^2\eta I^2(t)S(t)\left(\frac{1}{Q''(1-\varepsilon(t))}\frac{\dot{c}(t)}{c^2(t)} - \frac{\varepsilon^2(t)}{\eta}\right). \tag{17}$$

For no interior minimum to exist it is sufficient to show that $\ddot{I}(t)|_{\dot{I}(t)=0} < 0$ for all $t > 0$, which occurs precisely when (7) holds. □

Two remarks on (7) are in order. First, it follows from (16) that (7) holds if and only if

$$\frac{\dot{\varepsilon}(t)}{\varepsilon(t)} < -\frac{\dot{S}(t)}{S(t)} \,(= \beta I(t)\varepsilon(t)).$$

The left-hand side is the percentage increase in exposure, and the right-hand side is the conditional probability of infection. Second, when $Q(d) = \frac{1}{2}d^2$, since $Q''(d) = 1$, (7)

reduces to

$$\frac{\dot{c}(t)}{c^2(t)} < \frac{\varepsilon^2(t)}{\eta}.$$

Before proving Proposition 2, we provide three lemmas on which we will build and which can be of independent interest. The first lemma shows that if the exposure level is positive at some point in time, it remains positive in the future. The second lemma shows that in our prudent distancing fatigue model, the distancing cost can attain a local maximum only while the prevalence is decreasing. The third lemma asserts that, at any local maximum of I, either the prevalence I is locally constant or I peaks (i.e., attains a strict local maximum).

Lemma 2. *In equilibrium, if $\varepsilon(t') > 0$ for some t', then $\varepsilon(t) > 0$ for all $t \geq t'$.*

Proof. Suppose, to the contrary, that individuals choose $\varepsilon(t) = 0$ for some $t > t'$, and let $\underline{t} := \inf\{t \geq t' \mid \varepsilon(t) = 0\}$. Since I and c are continuous in equilibrium, so is ε. Thus, $\varepsilon(\underline{t}) = 0$ and consequently $\underline{t} > t'$. Towards the contradiction we will argue that in any small enough left neighborhood of $\underline{t}$, $\dot{\varepsilon}(t) > 0$.

At any t where $\varepsilon(t) > 0$, ε is differentiable with derivative

$$\dot{\varepsilon}(t) = \frac{Q'(1-\varepsilon(t))}{Q''(1-\varepsilon(t))}\left(\frac{\dot{c}(t)}{c(t)} - \frac{\dot{I}(t)}{I(t)}\right). \tag{18}$$

In addition, $\varepsilon(t) > 0$ on $(\underline{t}, t')$ implies

$$\begin{aligned} c(t) - c_0 &= k\int_0^t e^{-r(t-\tau)} g(1-\varepsilon(\tau))d\tau \\ &< k\int_0^t e^{-r(t-\tau)} g(1)d\tau \\ &< \frac{k}{r}g(1). \end{aligned}$$

Since I and c are continuous in equilibrium, for any $\delta_1 > 0$, there exists $\delta_2 > 0$ such that $\varepsilon(t) < \delta_1$ if $t \in (\underline{t} - \delta_2, \underline{t}]$. But then, given that $c(t) - c_0 < \frac{k}{r}g(1)$, δ_1 can be chosen small enough so that $r(c(t) - c_0) < kg(1-\varepsilon(t))$. In other words, for δ_2 small enough, $\dot{c}(t) > 0$ for $t \in (\underline{t} - \delta_2, \underline{t})$. Moreover, equation (4) implies that $\dot{I} < 0$ whenever $\varepsilon < \frac{\gamma}{\beta}$. Therefore, δ_1 can be chosen so that $\dot{c}(t) > 0$ and $\dot{I}(t) < 0$. Consequently, due to (18), $\dot{\varepsilon}(t) > 0$ on $(\underline{t} - \delta_1, \underline{t})$. But this means that, whenever $\varepsilon(t)$ becomes very small, it starts increasing and thus cannot reach 0. □

Lemma 3. *Suppose c is given by (8) and $\dot{I}(0) > 0$. In equilibrium, if c attains a local maximum (minimum) at $t > 0$, then $\dot{I}(t) \leq 0$ (≥ 0).*

Proof. As $\dot{I}(0) > 0$, it must be the case that $\varepsilon(0) > 0$. By Lemma 2, $\varepsilon(t) > 0$ for all $t \geq 0$. By implication ε and therefore $\dot{c}$ are differentiable for all $t > 0$.

Suppose c attains a critical point at some t. Thus, $\dot{c}(t) = 0$. Differentiating (10) and evaluating it at $\dot{c}(t) = 0$ yields

$$\begin{aligned}\ddot{c}(t)|_{\dot{c}(t)=0} &= -kg'(1-\varepsilon(t))\dot{\varepsilon}(t) \\ &= kg'(1-\varepsilon(t))\frac{Q'(1-\varepsilon(t))}{Q''(1-\varepsilon(t))}\frac{\dot{I}(t)}{I(t)}.\end{aligned}$$

Thus, if c attains a local maximum (minimum) at t, it is necessary that $\dot{I}(t) \leq 0$ (≥ 0). □

Lemma 4. *If I attains a local maximum at t_0, then there exists $\delta \in (0, t_0)$ satisfying one (and only one) of the following properties: (i) I is locally constant, i.e., $I(t) = I(t_0)$ for all $t \in (t_0 - \delta, t_0 + \delta)$; or (ii) $I(t_0)$ is a strict local maximum, i.e., $I(t) < I(t_0)$ for all $t \in (t_0 - \delta, t_0 + \delta)$.*

Proof. Suppose that I attains a local maximum at t_0. Since $\dot{I}(0) > 0$, it follows that $\varepsilon(0) > 0$. By Lemma 2, $\varepsilon(t) > 0$ for all $t > 0$. As a consequence, $\dot{I}(\cdot)$ is differentiable.

Since $\varepsilon(t) > 0$ for all $t > 0$, the SIR dynamics are characterized as follows:

$$\begin{aligned}\dot{S}(t) &= -\beta S(t)I(t)\left(1-(Q')^{-1}\left(\frac{\eta\beta I(t)}{c(t)}\right)\right), \\ \dot{I}(t) &= \beta S(t)I(t)\left(1-(Q')^{-1}\left(\frac{\eta\beta I(t)}{c(t)}\right)\right) - \gamma I(t), \\ \dot{R}(t) &= \gamma I(t), \\ \dot{c}(t) &= kg\left((Q')^{-1}\left(\frac{\eta\beta I(t)}{c(t)}\right)\right) - r(c(t)-c_0).\end{aligned}$$

Since Q is analytic, Q' is analytic (e.g., Krantz and Parks (2002, Proposition 1.1.14)). Since $(Q')^{-1}\left(\frac{\eta\beta I(\cdot)}{c(\cdot)}\right) \in (0,1)$, it follows from the inverse function theorem that $(Q')^{-1}\left(\frac{\eta\beta I(\cdot)}{c(\cdot)}\right)$ is analytic (e.g., Krantz and Parks (2002, Theorem 1.5.3)). Also, g is analytic. Then, since the function that determines the right-hand sides of the above system of ordinary differential equations is an analytic function of (S, I, R, c), the solution (S, I, R, c) is analytic (e.g., see Tenenbaum and Polland (1985, Theorem 38.14)).[29] Consequently, I is an analytic function.

Since I is analytic, there exists $\delta \in (0, t_0)$ such that either (i) $I(t) = I(t_0)$ for all $t \in (t_0 - \delta, t_0 + \delta)$ or (ii) I does not have any stationary point in $(t_0 - \delta, t_0 + \delta) \setminus \{t_0\}$.[30]

[29] This is an ordinary-differential-equation version of the more general Cauchy-Kovalevskaya theorem.

[30] The latter property is referred to as the principle of isolated zeros and is a special case of the identity

In the latter case, since I is analytic, it is Taylor-approximated by

$$I(t_0) + \frac{I^{(k)}(t_0)}{k!}(t - t_0)^k,$$

where $k > 1$ is the smallest natural number satisfying $\frac{I^{(k)}(t_0)}{k!} \neq 0$. Since I attains a local maximum at t_0, k is even. Then, I attains a strict local maximum, as desired. □

Proof of Proposition 2. The proof proceeds in three steps.

Step 1. Since $\dot{I}(0) > 0$ and $I_\infty = 0$, it follows that I has at least one local maximum. Let t_1 be some t at which a local maximum of I is attained. Thus, $\dot{I}(t_1) = 0$ and $\ddot{I}(t_1) \leq 0$; differentiability of $\dot{I}$ is established in the proof of Lemma 4. Then by (17) in the proof of Lemma 1, it must be the case that

$$\frac{1}{Q''(1 - \varepsilon(t_1))} \frac{\dot{c}(t_1)}{c^2(t_1)} \leq \frac{\varepsilon^2(t_1)}{\eta}.$$

To show that $I(t_1)$ is the unique strict local maximum (i.e., the single peak), suppose by contradiction that there exist $t_3 > t_1$ such that $\dot{I}(t_3) = 0$ and $\ddot{I}(t_3) \leq 0$. Then, by Lemma 4, one of the following holds: (i) $I(t_1)$ is not a strict local maximum, in which case it is locally constant; or (ii) there exists another strict local maximum. In either case, there exists $t_2 > t_1$ such that $\dot{I}(t) \leq 0$ for all $t \in [t_1, t_2]$ and and $\ddot{I}(t_2) \geq 0$. In case (ii), this follows from the fact that there has to be a local minimum between two strict local maxima.

We consider two cases. First, suppose $c(t_2) \geq c(t_1)$. Then:

$$\begin{aligned}
\dot{c}(t_2) &= kg(1 - \varepsilon(t_2)) - r(c(t_2) - c_0) \\
&< kg(1 - \varepsilon(t_1)) - r(c(t_1) - c_0) \\
&= \dot{c}(t_1),
\end{aligned}$$

where the inequality follows from the fact that at any t such that $\dot{I}(t) = 0$, $\varepsilon(t) = \gamma/(\beta S(t))$ and that $S(t)$ is decreasing. Inequality $\varepsilon(t_1) < \varepsilon(t_2)$ together with the assumption $Q''' \leq 0$ implies $Q''(1 - \varepsilon(t_1)) \leq Q''(1 - \varepsilon(t_2))$. As a consequence,

$$\frac{1}{Q''(1 - \varepsilon(t_2))} \frac{\dot{c}(t_2)}{c^2(t_2)} < \frac{1}{Q''(1 - \varepsilon(t_1))} \frac{\dot{c}(t_1)}{c^2(t_1)} \leq \frac{\varepsilon^2(t_1)}{\eta} < \frac{\varepsilon^2(t_2)}{\eta},$$

theorem for (real) analytic functions. This statement follows from Krantz and Parks (2002, Corollary 1.2.7).

which, due to equality (17) in the proof of Lemma 1, contradicts $\dot{I}(t_2) = 0$ and $\ddot{I}(t_2) \geq 0$.

Second, suppose $c(t_2) < c(t_1)$. By the definition of t_2, I is weakly decreasing on $[t_1, t_2]$. Since c is continuous on $[t_1, t_2]$, it attains a maximum and minimum on the interval by the extreme value theorem. Lemma 3 implies that if c attains an interior extremum, then it has to be a local maximum. Alternatively, c is decreasing on the whole interval. In either case $\dot{c}(t_2) \leq 0$. But then the inequality $\frac{1}{Q''(1-\varepsilon(t_2))}\frac{\dot{c}(t_2)}{c^2(t_2)} < \frac{\varepsilon^2(t_2)}{\eta}$ is automatically satisfied and thus $\ddot{I}(t_2) < 0$, which contradicts the supposition. Thus, I is single peaked, as desired.

Step 2. First, since $\dot{c}(0) = kg(1-\varepsilon(0)) > 0$, there exists t_1 such that $c(t_1) > c_0$. Otherwise, $\dot{c}(0) \leq 0$, a contradiction. Since $r > 0$ and $\lim_{t\to\infty} \varepsilon(t) = 1$, it follows that $\lim_{t\to\infty} c(t) = c_0$. Thus, there exists $t_2 \geq t_1$ such that $c(t) \leq c(t_1)$ for all $t \geq t_2$. Now, c admits a local maximum on $[0, t_2]$ by the extreme value theorem. By construction, the local maximum of c on $[0, t_2]$ is a local maximum on $[0, \infty)$.

Second, a proof almost identical to that of Lemma 4 shows that either $c(t_0)$ is a strict local maximum or otherwise c is locally constant at t_0. In either case, suppose to the contrary that there would exist t_1 and t_2 such that $t_1 < t_2$ and $c'(t_1) = c'(t_2) = 0$. Since c is continuous, it has a minimum on the interval $[t_1, t_2]$ by the extreme value theorem. Let $\tilde{t} \in (t_1, t_2)$ be some t at which c is minimized over $[t_1, t_2]$. Then $\dot{c}(t_1) = \dot{c}(\tilde{t}) = \dot{c}(t_2) = 0$. Using equation (10), we obtain

$$g(1-\varepsilon(t)) = \frac{r}{k}(c(t) - c_0) \text{ for } t \in \{t_1, \tilde{t}, t_2\}.$$

As $r > 0$, the inequality $c(\tilde{t}) \leq \min(c(t_1), c(t_2))$ implies that $1-\varepsilon(\tilde{t}) \leq \min(1-\varepsilon(t_1), 1-\varepsilon(t_2))$. In turn, the last two inequalities together with (6) imply that $I(\tilde{t}) \leq \min(I(t_1), I(t_2))$, which would contradict that I is single-peaked as established in Proposition 2.

Step 3. The third part of the proposition follows from the previous parts and Lemma 3. □

Proof of Proposition 3. Take c, t, and c_2 as in the statement of the proposition. Suppose that $c_2(t) = \bar{c}(t)$. Let $(S_2, I_2, R_2, c_2, \varepsilon_2)$ be the equilibrium under c_2. By the definition of the equilibrium, S_2 and I_2 are continuous. Notice that S_2 and I_2 coincide with S and I on $[0, t]$.

If c_2 has any discontinuities at some $\tau > t$, let t' be smallest $\tau > t$ where c_2 is discontinuous; otherwise set $t' = \infty$. Since S_2 and I_2 are continuous, it follows from (3)

and (4) that $\dot{S}_2$ and $\dot{I}_2$ exist and are continuous on (t, t'). Notice that

$$\beta\varepsilon_2(t)S_2(t) - \gamma = 0.$$

By continuity of ε_2 and S_2 for every $\delta_1 > 0$ there exists $\delta_2 > 0$ such that $|\varepsilon_2(t)S_2(t) - \varepsilon_2(s)S_2(s)| < \delta_1$ for all s such that $|s - t| < \delta_2$. Consequently,

$$\begin{aligned}\dot{I}_2(\tau) &= I_2(\tau)(\beta\varepsilon_2(\tau)S_2(\tau) - \gamma)\\ &< I_2(\tau)(\beta\varepsilon_2(t)S_2(t) + \delta_1 - \gamma)\\ &= \delta_1 I_2(\tau),\end{aligned}$$

for all $\tau \in (t, t + \delta_2)$. Therefore the right limit of $\dot{I}_2(\tau)$ at t is 0. It is then easy to see that if $c_2(t) < \bar{c}(t)$ the derivative of I_2 would be smaller than 0. □

B Far-sighted Decision-Making

We present a model with far-sighted decision-making, and provide numerical support for our main insights. Hence, the assumption of myopic decision-making is not the main driver of our findings.

As before, the individuals at each point in time decide the level of distancing, which determines the likelihood of infection. An individual's flow payoff from being in state $\theta \in \{S, I, R\}$ is π_θ. We assume $\pi_S \geq \pi_R \geq \pi_I$.[31] The individual discounts the future at rate $\rho > 0$.

A susceptible individual i with exposure $\varepsilon_i(t)$ enjoys the instantaneous payoff $\pi_S - \frac{c_i(t)}{2}(1 - \varepsilon_i(t))^2$, i.e., we assume $Q(d_i) = \frac{1}{2}d_i^2$. For ease of exposition, here we suppose that $\dot{c}_i(t)$ does not depend on the current distancing $1 - \varepsilon_i(t)$ in (1), i.e., we suppose that the susceptible individual i takes the distancing cost function c_i as given when she decides her exposure. This is because the main insight that the effectiveness of future mitigation-policies decline after introducing a current policy holds under no distancing fatigue.[32]

[31] Models with endogenous cost of infection have been presented in Reluga (2010), Fenichel et al. (2011), Fenichel (2013), Toxvaerd (2020), McAdams, Song, and Zou (2023), among others. Yet, analytical characterizations of equilibria even with constant distancing cost are rather elusive.

[32] As the analysis of distancing fatigue introduces an additional state variable and thus is complicated for far-sighted individuals, we focus on the case in which each individual takes c_i as exogenously given. Our numerical analyses confirm that our main insights carry over to far-sighted individuals. In fact, this shows an additional advantage of our myopic model when it comes to adding distancing fatigue.

Let $1 - p_i(t)$ be the probability of being susceptible at time t and, conversely, $p_i(t)$ the probability that an individual has become infected in the past. Then, $\dot{p}_i(t)$ represents the rate at which susceptible individuals become infected

$$\dot{p}_i(t) = \varepsilon_i(t)\beta I(t)(1 - p_i(t)),$$

with $p_i(0) = 0$. Since we model the behavior of susceptible individuals, the probability that they are infected at the outset is zero. Once an individual gets infected, her progression to recovery is independent of her behavior. Her continuation payoff from the moment she became infected is $V_I = \frac{1}{\rho+\gamma}\left(\pi_I + \frac{\gamma}{\rho}\pi_R\right)$.[33]

A susceptible individual who faces average exposure ε from her peers solves the problem

$$\max_{\varepsilon_i(\cdot)\in[0,1]} \int_0^\infty e^{-\rho t}\left\{(1 - p_i(t))[\pi_S - \frac{c_i(t)}{2}(1 - \varepsilon_i(t))^2] + p_i(t)\rho V_I\right\} dt \tag{19}$$

s.t.

$$\dot{p}_i(t) = \beta\varepsilon_i(t)I(t)(1 - p_i(t)),$$

$$p_i(0) = 0,$$

the underlying SIR dynamics given by equations (3), (4) and (5) with the initial condition $(S(0), I(0), R(0)) = (1 - I_0, I_0, 0)$ and $I_0 \in (0, 1)$, and the distancing cost function c_i satisfying (1), where $d_i = 1 - \varepsilon_i$ with $c_i(0) = c_0$.[34] The individual's payoff can be thought of as the expected value of being susceptible or infected at each point in time where the flow payoff of an infected individual is ρV_I.

We restrict attention to distancing cost functions c_i which satisfy

$$\pi_S - \sup_{t\in[0,\infty)} \frac{c_i(t)}{2} > \rho V_I. \tag{20}$$

This assumption states that even if a susceptible individual is fully distancing, her flow payoff of being suceptible is greater than the flow payoff of being infected.

An equilibrium $(S, I, R, c, \varepsilon, p)$ of the far-sighted decision-making model is defined analogously to our main model. Note that, in equilibrium, each p_i is determined by ε, I, and c, and thus $p = p_i$ for each i. The cost of infection $\eta = \eta_i$, which is the co-state variable associated with the individual problem, changes over time. While (S, I, R, c)

[33] See Carnehl, Fukuda, and Kos (2023, Remark 1) for the formal derivation of V_I.

[34] Note that here we suppose that the individual i treats c_i as given. When $\dot{c}_i$ depends on $1 - \varepsilon_i(t)$, we need to incorporate the law of motion for c_i into the problem. Again, our assumption makes it easier to analyze the time-varying distancing costs for far-sighted individuals.

is solved forward, η is solved backward. Hence, analytically characterizing the set of equilibria is untenable.

To characterize the forward-looking variable η, we set up the current-value Hamiltonian of problem (19):

$$\mathcal{H}_i = (1 - p_i(t))[\pi_S - \frac{c_i(t)}{2}(1 - \varepsilon_i(t))^2] + p_i(t)\rho V_I - \eta_i(t)\beta\varepsilon_i(t)I(t)(1 - p_i(t)),$$

where $\eta_i(t)$ is the current-value co-state variable. It represents the marginal cost of an increase in the probability of being infected at time t. The optimality condition with respect to exposure $\varepsilon_i(t)$ at time t is

$$\frac{\partial \mathcal{H}_i}{\partial \varepsilon_i(t)} = (1 - p_i(t))[c_i(t)(1 - \varepsilon_i(t)) - \beta\eta_i(t)I(t)] = 0.$$

Thus, the optimality condition delivers equilibrium distancing

$$d_i(t) = \frac{\beta\eta_i(t)I(t)}{c_i(t)}, \tag{21}$$

provided that the entire distancing path admits an interior solution, i.e., that $d_i(t) \in [0, 1]$ for all t. One should keep in mind that the marginal cost of an increased probability of infection, $\eta_i(t)$, is positive due to the assumption given by (20). The current-value co-state variable η_i follows the adjoint equation

$$\begin{aligned}\dot{\eta}_i(t) &= \rho\eta_i(t) + \frac{\partial \mathcal{H}_i}{\partial p_i(t)} \\ &= \eta_i(t)\left(\rho + \varepsilon_i(t)\beta I(t)\right) + \left(\pi_S - \frac{c_i(t)}{2}(1 - \varepsilon_i(t))^2 - \rho V_I\right).\end{aligned}$$

The transversality condition is $\lim_{t\to\infty} e^{-\rho t}\eta_i(t) = 0$. In equilibrium, $\eta = \eta_i$ for all i.

Using the adjoint equation and the transversality condition, we can solve for η.

Lemma 5. *Suppose that the rest of the population is following the strategy ε, and ε_i is the individual i's best response. Then*

$$\eta_i(t) = \int_t^\infty e^{-\rho(s-t)}\frac{1 - p_i(s)}{1 - p_i(t)}\left(\pi_S - \frac{c_i(t)}{2}(1 - \varepsilon_i(s))^2 - \rho V_I\right) ds.$$

Let $(S, I, R, \varepsilon, p)$ be an equilibrium. Then

$$\eta(t) = \int_t^\infty e^{-\rho(s-t)}\frac{S(s)}{S(t)}\left(\pi_S - \frac{c(s)}{2}(1 - \varepsilon(s))^2 - \rho V_I\right) ds.$$

The proof of this lemma is similar to that of Carnehl, Fukuda, and Kos (2023, Lemma 2), and thus it is omitted. Instead, we provide the interpretation of the lemma. We term $\pi_S - \frac{c(t)}{2}(1-\varepsilon(t))^2 - \rho V_I$ the *susceptibility premium* at time t. It is the difference in flow payoffs between being susceptible and being infected. The cost of getting infected, $\eta(t)$, is the discounted value of the susceptibility premium over time weighted by the conditional probability of being susceptible at each time in the future, $s \geq t$, $\frac{S(s)}{S(t)}$. Distancing over a period of time reduces the quality of life and, thus, the susceptibility premium. However, it also decreases the probability that the individual will get infected and rewards her with the premium for a longer period of time.

As in Carnehl, Fukuda, and Kos (2023, Lemma 3), one can also show that η is bounded. Letting $(S, I, R, c, \varepsilon, p)$ be an equilibrium,

$$\frac{\pi_S - \rho V_I - \frac{c(t)}{2}}{\rho + \beta} \leq \eta(t) \leq \frac{\pi_S - \rho V_I}{\rho} \text{ and } \lim_{t\to\infty} \eta(t) = \frac{\pi_S - \rho V_I}{\rho}.$$

As time passes, η eventually converges to the upper bound, which is attained when individuals choose full exposure in perpetuity without facing any risk of becoming infected. This is the case in which getting infected would be most costly as there is no need to distance and no risk of future infection. The convergence to this bound is intuitive, because the disease dies out and obviates the need for distancing in the limit as time goes to infinity.

Below, we present the results of our numerical simulations with endogenous η. We calibrate the parameters for the beginning of COVID-19. The value of η in the main text corresponds to the upper bound $\eta = \frac{\pi_S - \rho V_I}{\rho}$.[35] For the values of π_S, ρ, and V_I, see Carnehl, Fukuda, and Kos (2023).

Specifically, we revisit Example 1 with endogenous η. To that end, we define

$$\overline{c}(t) := \begin{cases} \frac{\beta^2 I(t) S(t) \eta(t)}{\beta S(t) - \gamma}, & \text{if } S(t) > \frac{\gamma}{\beta} \\ \infty, & \text{if } S(t) \leq \frac{\gamma}{\beta} \end{cases}.$$

Note that the only difference from the main text is that η is now time-varying. This is because the exposure level of the far-sighted individual is $\varepsilon(t) = 1 - \frac{\beta \eta(t) I(t)}{c(t)}$. One can show that Proposition 3 holds under this setting, as the proof in Appendix A simply extends to this case.

[35] Hence, by assumption, in our numerical simulations of the model in which η is fixed at the upper bound, individuals engage distancing more and the prevalence is lower. In contrast, by taking the lower bound of η, we can also bound the prevalence from above. This way, the model with constant infection cost can also shed light on the dynamics of the model with endogenous infection cost.

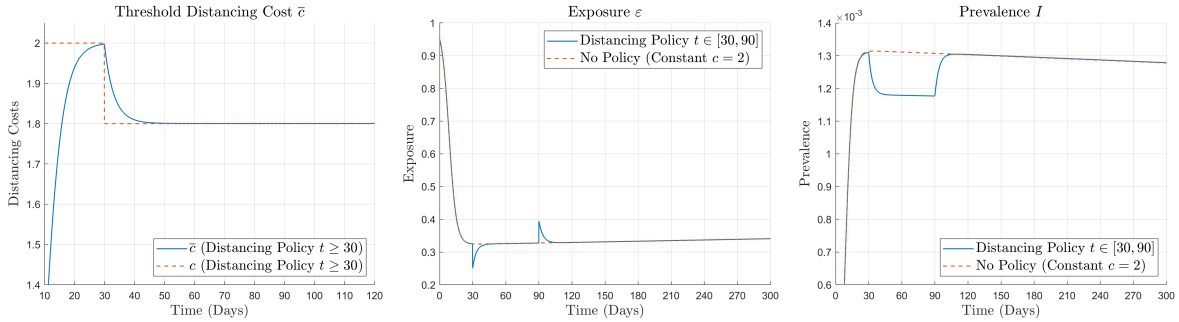

Figure 3: *Social-Distancing Policy.* The left panel depicts the threshold distancing cost function $\bar{c}$ over time. The central panel depicts the exposure level ε over time. The right panel depicts the prevalence I over time.

The left panel of Figure 3 illustrates the threshold distancing function $\bar{c}$. Figure 3 look similar to Figure 1.

To sum up, while one might argue that individuals do not fully discount the future, the difficulty in predicting the path of an epidemic might induce them to simply respond to the current state of the epidemic. In addition, analytical results for the SIR model with endogenous distancing by far-sighted individuals are few and far between.[36] The myopic model enables one to provide analytical insights and pave the road towards the understanding of the model with far-sighted individuals. Moreover, our numerical analysis highlights that assuming a fixed cost of infection is not the main driver of our findings.

C Parameter Assumptions

This appendix outlines the assumptions imposed on the parameters $(\beta, \gamma, I_0, \pi_S, c_0, \eta)$. Table 1 reports the calibration values, the majority of which are taken from Farboodi et al. (2021). Under these assumptions, we solve the model numerically using a fourth-order Runge–Kutta method.

First, assuming that the average length of disease is 7 days, we take the recovery rate $\gamma = 1/7$. Second, we set the transmission rate β in a way such that, in the benchmark standard SIR model, the initial growth rate $\frac{\dot{I}(0)}{I(0)}$ is approximately 0.3 given $S_0 \approx 1$. Thus, we set $\beta = 0.3 + \gamma = 0.443$. Third, for the initial seed of infections I_0, we match 194 people who deceased from COVID-19 in the US on or prior to March 18, a week after the pandemic declaration by the WHO on March 11, 2020. Given a population of 328

[36] In the context of behavioral SIR models, it has not even been established whether such a model with equilibrium distancing has a single peak even for the case in which distancing cost is constant over time. For example, in an optimal planner problem of distancing, Kruse and Strack (2023) show that the prevalence peaks at most twice.

Table 1: *Baseline Parameters for Numerical Analysis.*

Parameter	Description	Value	Source
γ	Recovery Rate	$1/7$	Farboodi et al. (2021)
β	Transmission Rate	$0.3+\gamma$	Farboodi et al. (2021)
I_0	Initial Seed of Infections	0.95×10^{-4}	Based on death toll in the US before March 19, 2020
c_0	Initial Distancing Cost	2	Carnehl et al. (2023)
π_S	Flow Payoff of Susceptibles	0	Carnehl et al. (2023)
η	Cost of Infection	2761.63	Hall et al. (2020)

million and an IFR of 0.0062, we let $I_0 = 0.95 \times 10^{-4}$.

Fourth, we follow Carnehl, Fukuda, and Kos (2023) and set the flow payoff of susceptibles $\pi_S = 0$. Fifth, since we specify $Q(1-\varepsilon(t)) = \frac{1}{2}(1-\varepsilon(t))^2$ in our numerical simulation, and choose the initial distancing cost to $c_0 = 2$ as in Carnehl, Fukuda, and Kos (2023).

Sixth, to compute the cost of infection η, we follow the same steps as in Farboodi et al. (2021). Namely, we assume the value of a statistical year of life to be US$ $270,000$ and an average remaining life expectancy of COVID-19 victims to be 14.5 years, which gives US$ $3,915,000$ where the numerical values are taken from Hall et al. (2020). To avoid a 0.1 percent probability of death, an individual would be willing to pay US$ $0.001 \times 3,915,000$. Following Alvarez et al. (2021) and Farboodi et al. (2021), we use the discount rate of $\rho = (0.05+0.67)/365$, which consists of a 5 percent annual discount rate and an expected time of 1.5 years until the arrival of a cure. Then, an individual is willing to pay US$ $\rho \cdot 3,915$ to avoid the 0.1 percent probability of death. Using the US per capita consumption from Hall et al. (2020) of US$ 45,000 per year, an individual is willing to give up $\frac{3{,}915\rho \cdot 365}{45{,}000} = 31.755\rho$ in terms of annual consumption units, i.e., $\varepsilon = 1 - 31.755\rho$, to avoid a 0.1 percent risk of death. Applying the distancing cost function $\frac{c_0}{2}(1-\varepsilon)^2$ evaluated at c_0, an individual is indifferent between 31.755 ρ units of consumption per period and full exposure with a 0.001 risk of death, which has a utility cost of v:

$$-\frac{(1-1)^2}{\rho} - 0.001v = -\frac{(1-31.755\rho)^2}{\rho}.$$

Multiplying this value of life in utils by the death rate of 0.0062 (also from Hall et al., 2020) yields a cost of infection $\eta = 2761.63$.

For the extended model in Appendix B, we additionally set $\pi_R = 0$ and $\pi_I = -399.96$ so that $V_I = \frac{\pi_I}{\rho+\gamma} = -\eta$ works as the upper bound of $\eta(t)$. We set the terminal condition $\eta(T) = \frac{\pi_S - \rho V_I}{\rho}$ at $T = 400 \times 365$ (days).

References

Acemoglu, D., V. Chernozhukov, I. Werning, and M. D. Whinston (2021): "Optimally Targeted Lockdowns in a Multi-group SIR Model," *American Economic Review: Insights*, 3, 487–502.

Adda, J., R. Boucekkine, and J. Thuilliez (2024): "Epidemics, Mental Health and Public Trust," Working paper.

Alvarez, F., D. Argente, and F. Lippi (2021): "A Simple Planning Problem for COVID-19 Lock-down, Testing, and Tracing," *American Economic Review: Insights*, 3, 367–82.

Atkeson, A. G., K. Kopecky, and T. Zha (2021): "Behavior and the Transmission of COVID-19," *AEA Papers and Proceedings*, 111, 356–360.

Avery, C. (2024): "The Economics of Social Distancing and Vaccination," *Review of Economic Design*, 28, 781–812.

Baucells, M. and L. Zhao (2019): "It is Time to Get Some Rest," *Management Science*, 65, 1717–1734.

Baumeister, R. F. and M. R. Leary (1995): "The Need to Belong: Desire for Interpersonal Attachments as a Fundamental Human Motivation," *Psychological Bulletin*, 117, 497–529.

Bootsma, M. C. J. and N. M. Ferguson (2007): "The Effect of Public Health Measures on the 1918 Influenza Pandemic in U.S. Cities," *Proceedings of the National Academy of Sciences of the United States of America*, 104, 7588–7593.

Bowlby, J. (1969): *Attachment and Loss: Volume I: Attachment*, Basic Books.

Brauer, F. and C. Castillo-Chavez (2012): *Mathematical Models in Population Biology and Epidemiology*, Springer, second ed.

Brett, T. S. and P. Rohani (2020): "Transmission Dynamics Reveal the Impracticality of COVID-19 Herd Immunity Strategies," *Proceedings of the National Academy of Sciences*, 117, 25897–25903.

Budish, E. (2025): "$R < 1$ as an Economic Constraint," *Review of Economic Design*, 29, 9–43.

Caley, P., D. J. Philp, and K. McCracken (2008): "Quantifying Social Distancing Arising from Pandemic Influenza," *Journal of the Royal Society Interface*, 5, 631–639.

Carnehl, C., S. Fukuda, and N. Kos (2023): "Epidemics with Behavior," *Journal of Economic Theory*, 207, 105590.

Chakrabarti, S., I. Krasikov, and R. Lamba (2022): "Behavioral Epidemiology: An Economic Model to Evaluate Optimal Policy in the Midst of a Pandemic," Working paper.

Chen, F. (2012): "A Mathematical Analysis of Public Avoidance Behavior during Epidemics Using Game Theory," *Journal of Theoretical Biology*, 302, 18–28.

Cochrane, J. H. (2020): "An SIR Model with Behavior," Https://johnhcochrane.blogspot.com/2020/05/an-sir-model-with-behavior.html.

Dasaratha, K. (2023): "Virus dynamics with behavioral responses," *Journal of Economic Theory*, 214, 105739.

Droste, M. and J. H. Stock (2021): "Adapting to the COVID-19 Pandemic," *AEA Papers and Proceedings*, 111, 351–355.

Du, Z., L. Wang, S. Shan, D. Lam, T. K. Tsang, J. Xiao, H. Gao, B. Yang, S. T. Ali, S. Pei, I. C.-H. Fung, E. H. Y. Lau, Q. Liao, P. Wu, L. A. Meyers, G. M. Leung, and B. J. Cowling (2022): "Pandemic fatigue impedes mitigation of COVID-19 in Hong Kong," *Proceedings of the National Academy of Sciences*, 119, e2213313119.

Eisenberger, N. I. (2012): "The pain of social disconnection: examining the shared neuralunderpinnings of physical and social pain," *Nature Reviews Neuroscience*, 13, 421–434.

Engle, S., J. Keppo, M. Kudlyak, E. Querciolo, L. Smith, and A. Wilson (2021): "The Behavioral SIR Model, with Applications to the Swine Flu and COVID-19 Pandemics," Working paper.

Farboodi, M., G. Jarosch, and R. Shimer (2021): "Internal and External Effects of Social Distancing in a Pandemic," *Journal of Economic Theory*, 196, 105293.

Fenichel, E. P. (2013): "Economic Considerations for Social Distancing and Behavioral Based Policies during an Epidemic," *Journal of Health Economics*, 32, 440–451.

Fenichel, E. P., C. Castillo-Chavez, M. G. Ceddia, G. Chowell, P. A. G. Parra, G. J. Hickling, G. Holloway, R. Horan, B. Morin, C. Perrings, M. Springborn, L. Velazquez, and C. Villalobos (2011): "Adaptive Human Behavior in Epidemiological Models," *Proceedings of the National Academy of Sciences*, 108, 6306–6311.

Franzen, A. and F. Wöhner (2021): "Fatigue during the COVID-19 Pandemic: Evidence of Social Distancing Adherence from a Panel Study of Young Adults in Switzerland," *PLOS ONE*, 16, e0261276.

Giannitsarou, C., S. Kissler, and F. Toxvaerd (2021): "Waning Immunity and the Second Wave: Some Projections for SARS-CoV-2," *American Economic Review: Insights*, 3, 321–38.

Goldstein, P., E. L. Yeyati, and L. Sartorio (2021): "Lockdown Fatigue: The Diminishing Effects of Quarantines on the Spread of COVID-19," Working paper.

Goodkin-Gold, M., M. Kremer, C. M. Snyder, and H. Williams (2024): "Optimal Vaccine Subsidies for Epidemic Diseases," *Review of Economics and Statistics*, 106, 895–909.

Gualtieri, A. F. and P. Hecht (2021): "SARS-COV-2 Spread and Quarantine Fatigue: A Theoretical Model," Working paper.

Hall, R. E., C. I. Jones, and P. J. Klenow (2020): "Trading Off Consumption and COVID-19 Deaths," Working paper.

Harlow, H. F. and R. R. Zimmermann (1959): "Affectional response in the infant monkey: Orphaned baby monkeys develop a strong and persistent attachment to inanimate surrogate mothers," *Science*, 130, 421–432.

Hatchett, R. J., C. E. Mecher, and M. Lipsitch (2007): "Public health interventions and epidemic intensity during the 1918 influenza pandemic," *Proceedings of the National Academy of Sciences*, 104, 7582–7587.

Joshi, Y. V. and A. Musalem (2021): "Lockdowns lose one third of their impact on mobility in a month," *Scientific Reports*, 11, 1–10.

Kermack, W. O. and A. G. McKendrick (1927): "A Contribution to the Mathematical Theory of Epidemics," *Proceedings of the Royal Society A: Mathematical, Physical and Engineering Sciences*, 115, 700–721.

Krantz, S. G. and H. R. Parks (2002): *A Primer of Real Analytic Functions*, Birkhäuser, second ed.

Kruse, T. and P. Strack (2023): "Optimal Dynamic Control of an Epidemic," *Operations Research*, 72, 1031–1048.

MacDonald, J. C., C. Browne, and H. Gulbudak (2021): "Modeling COVID-19 Outbreaks in United States with Distinct Testing, Lockdown Speed and Fatigue Rates," Working paper.

Matthews, G. A., E. H. Nieh, C. M. Vander Weele, S. A. Halbert, R. V. Pradhan, A. S. Yosafat, G. F. Glober, E. M. Izadmehr, R. E. Thomas, L. Gabrielle D., C. P. Wildes, M. A. Ungless, and K. M. Tye (2016): "Dorsal Raphe Dopamine Neurons Represent the Experience of Social Isolation," *Cell*, 164, 617–631.

McAdams, D. (2021): "The Blossoming of Economic Epidemiology," *Annual Review of Economics*, 13.

McAdams, D. and T. Day (2025): "The Political Economy of Epidemic Management," *Review of Economic Design*, 29, 115–148.

McAdams, D., Y. Song, and D. Zou (2023): "Equilibrium Social Activity during an Epidemic," *Journal of Economic Theory*, 207, 105591.

Meacci, L. and M. Primicerio (2021): "Pandemic Fatigue Impact on COVID-19 Spread: A Mathematical Modelling Answer to the Italian Scenario," *Results in Physics*, 31, 104895.

Nguyen, T. D., S. Gupta, M. Andersen, A. Bento, K. I. Simon, and C. Wing (2020): "Impacts of State Reopening Policy on Human Mobility," Working paper.

Petherick, A., R. Goldszmidt, E. B. Andrade, R. Furst, T. Hale, A. Pott, and A. Wood (2021): "A Worldwide Assesment of Changes in Adherence to COVID-19 Protective Behaviours and Hypothesized Pandemic Fatigue," *Nature Human Behavior*, 5, 1145–1160.

Rachel, L. (2025): "The Second Wave," *Review of Economic Design*, 29, 87–113.

Reluga, T. C. (2010): "Game Theory of Social Distancing in Response to an Epidemic," *PLoS Computational Biology*, 6.

Ross, R. and H. P. Hudson (1917): "An Application of the Theory of Probabilities to the Study of a Priori Pathometry.—Part III," *Proceedings of the Royal Society A: Mathematical, Physical and Engineering Sciences*, 93, 225–240.

Tenenbaum, M. and H. Polland (1985): *Ordinary Differential Equations*, Dover.

Toxvaerd, F. (2020): "Equilibrium Social Distancing," Working paper.

Walter, W. (1998): *Ordinary Differential Equations*, Springer.

Weitz, J. S., S. W. Park, C. Eksin, and J. Dushof (2020): "Awareness-Driven Behavior Changes Can Shift the Shape of Epidemics Away from Peaks and toward Plateaus, Shoulders, and Oscillations," *Proceedings of the National Academy of Sciences*, 117, 32764–32771.

WHO (2020): "Pandemic Fatigue-Reinvigorating the Public to Prevent COVID-19: Policy Framework for Supporting Pandemic Prevention and Management," .

Zhong, L., Y. Zhou, S. Gao, Z. Yu, Z. Ma, X. Li, Y. Yue, and J. Xia (2022): "COVID-19 Lockdown Introduces Human Mobility Pattern Changes for Both Guangdong-Hong Kong-Macao Greater Bay Area and the San Francisco Bay Area," *International Journal of Applied Earth Observation and Geoinformation*, 112, 102848.